Hindawi Publishing Corporation
Dataset Papers in Science
Volume 2014, Article ID 753131, 7 pages
http://dx.doi.org/10.1155/2014/753131

Dataset Paper

Dataset for Modelling Reaction Mechanisms Using Density Functional Theory: Mechanism of *ortho*-Hydroxylation by High-Valent Iron-Oxo Species

Azaj Ansari and Gopalan Rajaraman

Department of Chemistry, Indian Institute of Technology Bombay, Powai, Mumbai 400076, India

Correspondence should be addressed to Gopalan Rajaraman; rajaraman@chem.iitb.ac.in

Received 3 September 2013; Accepted 28 November 2013; Published 8 June 2014

Academic Editors: L. Bernasconi, H. Hirao, and J. Pons

Modelling reaction mechanisms using density functional theory is one of the popular routes to underpin the course of a chemical reaction. Although numerous publications have come out in this area, the pitfall of modelling such reactions and explicitly publishing the entire data set (structures, energies, coordinates, spin densities, etc.) which lead to the conclusions are scarce. Here we have attempted to set a trend wherein all the computed data to underpin the reaction mechanism of *ortho*-hydroxylation of aromatic compounds by high-valent iron-oxo complexes (Fe^{III}–OOH, Fe^{IV}=O, and Fe^{V}=O) are collected. Since the structure, energetics and other details of the calculations can be employed in future to probe/understand the reactivity pattern of such species, establishing the data set is justified. Here by analysing the presented results we also discuss in brief the presented results.

1. Introduction

Heme and nonheme metal catalytic reactions of aliphatic/aromatic hydrocarbons are an important tool in pharmaceutical industry [1, 2]. Iron catalyzed hydroxylations of organic compounds have been reported by several catalysts and studied by several experimentalists and theoreticians [3–8]. The Fe^{III}–OOH, Fe^{IV}=O, and Fe^{V}=O species are reported to be involved in the hydroxylation of aromatic and aliphatic compounds [3, 4]. At several instances, although the presence of Fe^{III}–OOH species has been directly detected, high-valent iron-oxo species are invoked to explain the reactivity of many mononuclear heme/nonheme iron enzymes. Particularly in the last decade the Fe^{IV}=O species are very popular as they have been hypothesized as potential oxidants in several aliphatic/aromatic hydroxylation reactions [9–13]. Besides the Fe^{IV}=O, the Fe^{V}=O intermediates also captured attention very recently in the hydroxylation reactions [3, 4] (Figure 2).

Detection of Fe^{V}=O species under ambient conditions is a challenging task and thus this species has been detected only at a few occasions [14–16]. Of particular interest here is the recently reported *ortho*-hydroxylation of aromatic compounds by a putative iron(V)-oxo species [3, 4]. In this dataset paper, we aim to list all the data which are collected over the years to underpin this reaction mechanism. In our original study [17], we use $[Fe^{II}(TPA)\ (CH_3CN)_2]^{2+}$ (tpa = tris(2-pyridylmethyl)amine) complex (shown in Figure 1) which performs *ortho*-hydroxylation very selectively [3]. Experimentally the mechanism of this regiospecific reaction is probed by various sets of tools such as spectroscopy and ^{18}O labelling experiments [3]. Since hydrogen peroxide is employed as the oxidant in this chemistry, the oxygen atom of the H_2O_2 is found to be incorporated in the product. The mechanistic study suggests the Fe^{III}–OOH species as an obvious starting point, but during the course of reaction, the Fe^{IV}=O and Fe^{V}=O species could in principle be generated, which then catalyze the reaction. These two species are generated by either homolytically or heterolytically cleaving the O–O bond of the Fe^{III}–OOH species (Figures 3, 4, and 5).

In our earlier mechanistic study we have modelled the reaction using DFT and assumed (i) Fe^{III}–OOH, (iv) Fe^{IV}=O, and (iii) Fe^{V}=O as the possible oxidants and also probed the

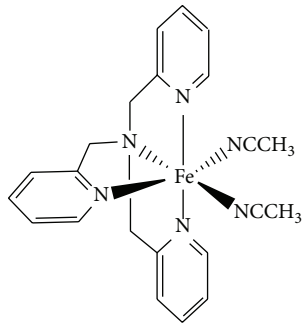

Figure 1: Schematic structure of complex $[Fe^{II}(TPA)(CH_3CN)_2]^{2+}$.

intrinsic mechanistic details on how each of these oxidants bifurcates as the reaction proceeds. The calculations were performed with B3LYP-D, B3LYP, wB97XD, B97D, M06-2X, OLYP, TPPSh, and MP2 functionals and the results within the employed functionals deviate to certain extent. As B3LYP-D is one of the state-of-the-art functionals, all the earlier results are discussed at this level and here we are presenting the employed dataset which leads to the mechanistic conclusions that this particular reaction is triggered specifically by an Fe^{V}=O species and that species prefers to undergo electrophilic attack to facilitate the hydroxylation reaction.

2. Methodology

All calculations were carried out by using the Gaussian 09 program [18]. The geometry optimizations have been performed initially using B3LYP [19, 20]. Basis set LanL2DZ for Fe [21–24] and a 6–31 G [25] basis set for the other atoms like C, H, N, and O are employed. Accuracy of B3LYP has been well documented by the work of Neese, Shaik, Siegbahn, Solomon, and Ryde earlier [26–32]. Many reported density functionals have issues of obtaining correct spin ground state. Some specific functionals such as OLYP [33] and TPSSh [34] are reported to predict correct spin state for iron complexes [35, 36]. However these functionals lack features like dispersion. Due to the absence of dispersion, the transition states are too loosely bound leading to the increase of the barrier heights. Dispersion corrected functionals such as M06-2X [37], B97D [38], and wB97XD address this issue to a certain extent [39], while addition of dispersion to the popular B3LYP (due to the work of Grimme) is found to be more robust and reliable [38, 40]. In case of iron-oxo complexes, B3LYP and B3LYP-D [38] along with TPSSh were reported to predict correct spin state in comparison to the CCSD(T) method [41].

Here we applied eight levels of theory (B3LYP, B3LYP-D, wB97XD, B97D, M06-2X, OLYP, TPPSh, and MP2 [42]) for the mechanistic study of *ortho*-hydroxylation reaction of the benzoic acid by using $[Fe^{III}(TPA)(OOH)]^{2+}$ catalyst (see Figure 1). We optimized all structures with B3LYP, B3LYP-D, B97D, wB97XD, and M06-2X and we also performed single point calculation with OLYP, TPSSh, and MP2 method on the B3LYP optimized geometries. With the exception of MP2, all methods support heterolytic cleavage. The performance of MP2 is the most unsatisfactory among the methods tested. This result is consistent with previous work indicating that high level quantum chemical methods (e.g., the spectroscopically oriented CI (SORCI) method of Neese [43]) fail to predict the correct ground state of Fe^{IV}=O species. Among the tested methods, our results illustrate that B3LYP, B3LYP-D, and wB97XD are consistently predicting the correct spin state compared to experimental data [3, 15]. Since the performances of all three functionals are nearly the same, here we intend to discuss B3LYP results, and comparison to other functionals has been made where appropriate.

3. Dataset Description

This Dataset Paper consists of 30 items which are described as follows.

Dataset Item 1 (Spectra). This computed energy profile for pathway I_a is optimized with B3LYP-D function. The computed values (ΔG) are given in kJ/mol.

Dataset Item 2 (Spectra). This computed energy profile for heterolytic cleavage of O–O bond of *cis*-Fe^{III}–OOH is optimized with B3LYP function. The computed values (ΔG) are given in kJ/mol.

Dataset Item 3 (Spectra). This computed energy profile for heterolytic cleavage of O–O bond of *cis*-Fe^{III}–OOH is optimized with B3LYP-D function. The computed values (ΔG) are given in kJ/mol.

Dataset Item 4 (Spectra). This computed energy profile for heterolytic cleavage of O–O bond of *cis*-Fe^{III}–OOH is optimized with B97D function. The computed values (ΔG) are given in kJ/mol.

Dataset Item 5 (Spectra). This computed energy profile for *ortho*-hydroxylation by C–H bond activation (pathway II_a) by Fe^{V}=O oxidant is optimized with B3LYP function. The computed values (ΔG) are given in kJ/mol.

Dataset Item 6 (Spectra). This computed energy profile for *ortho*-hydroxylation by C–H bond activation (pathway II_a) by Fe^{V}=O oxidant is optimized with B3LYP-D function. The computed values (ΔG) are given in kJ/mol.

Dataset Item 7 (Spectra). This computed energy profile for *ortho*-hydroxylation by C–H bond activation (pathway II_a) by Fe^{V}=O oxidant is optimized with wB97XD function. The computed values (ΔG) are given in kJ/mol.

Dataset Item 8 (Spectra). This computed energy profile for *ortho*-hydroxylation by C–H bond activation (pathway II_a) by Fe^{V}=O oxidant is optimized with B97D function. The computed values (ΔG) are given in kJ/mol.

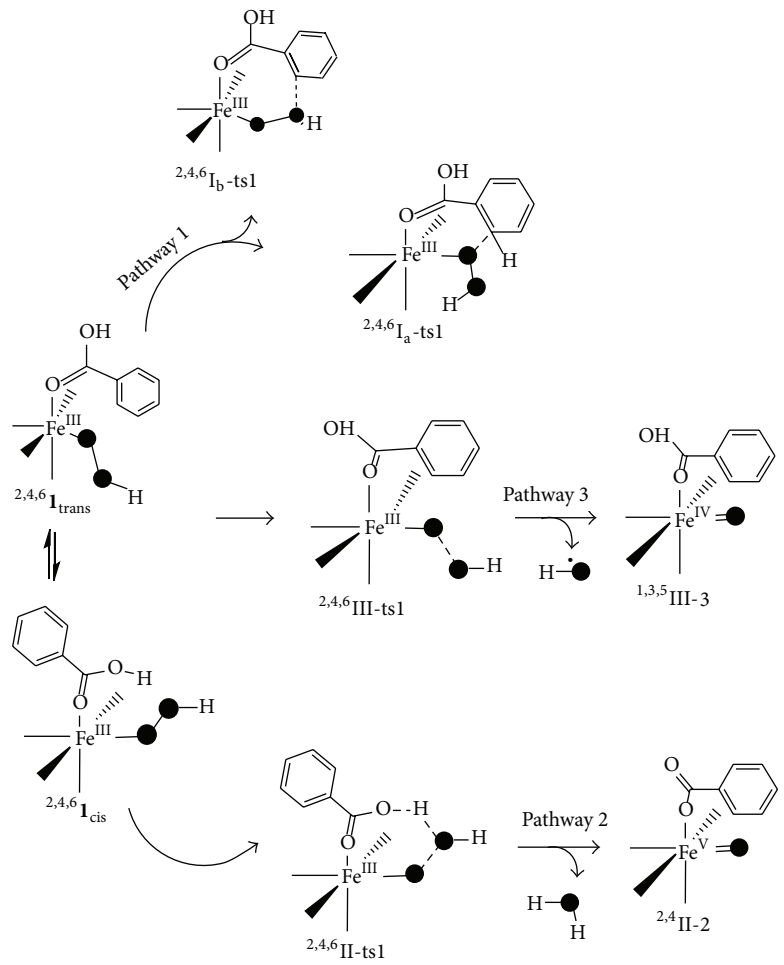

Figure 2: Schematic mechanism for the formation of intermediates Fe^{IV}=O and Fe^{V}=O species.

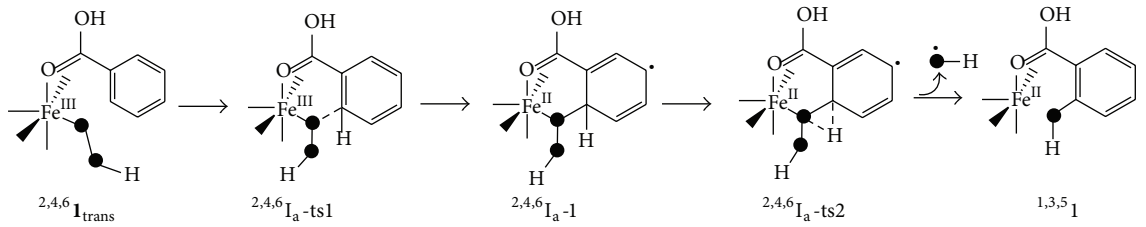

Figure 3: Schematic mechanism for the *ortho*-hydroxylation reaction by proximal oxygen attack by Fe^{III}–OOH species (pathway I_a).

Dataset Item 9 (Spectra). This computed energy profile for *ortho*-hydroxylation by C–H bond activation (pathway II_a) by Fe^{V}=O oxidant is optimized with M06-2X function. The computed values (ΔG) are given in kJ/mol.

Dataset Item 10 (Spectra). This computed energy profile for *ortho*-hydroxylation by electrophilic attack (pathway II_b) by Fe^{V}=O oxidant is optimized with B3LYP function. The computed values (ΔG) are given in kJ/mol.

Dataset Item 11 (Spectra). This computed energy profile for *ortho*-hydroxylation by electrophilic attack (pathway II_b) by Fe^{V}=O oxidant is optimized with B3LYP-D function. The computed values (ΔG) are given in kJ/mol.

Dataset Item 12 (Spectra). This computed energy profile for *ortho*-hydroxylation by electrophilic attack (pathway II_b) by Fe^{V}=O oxidant is optimized with wB97XD function. The computed values (ΔG) are given in kJ/mol.

Dataset Item 13 (Spectra). This computed energy profile for *ortho*-hydroxylation by electrophilic attack (pathway II_b) by Fe^{V}=O oxidant is optimized with B97D function. The computed values (ΔG) are given in kJ/mol.

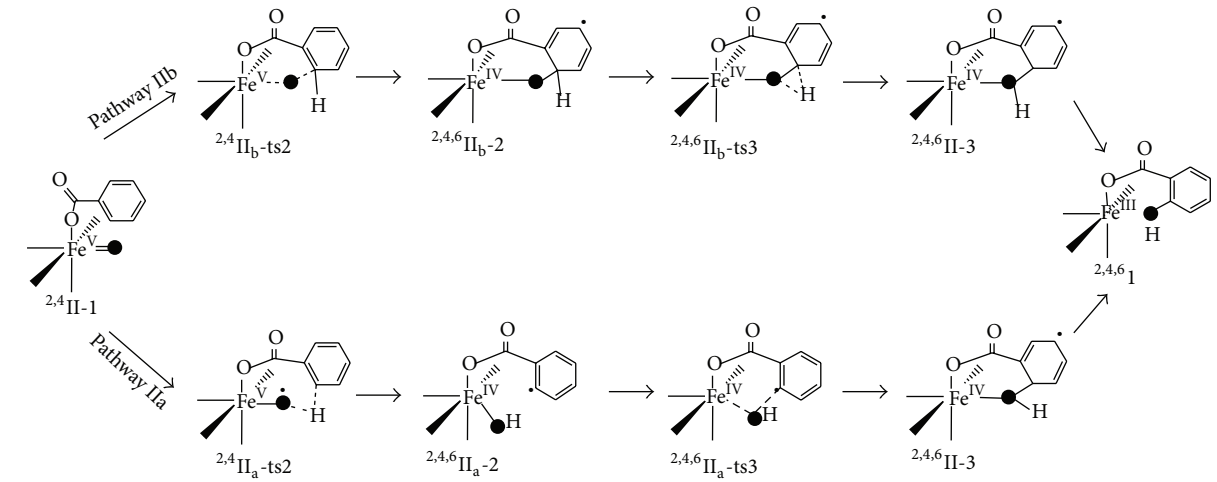

Figure 4: Schematic mechanism for the *ortho*-hydroxylation reaction by Fe^{V}=O oxidant where reaction may be proceeded via either C–H activation or electrophilic way.

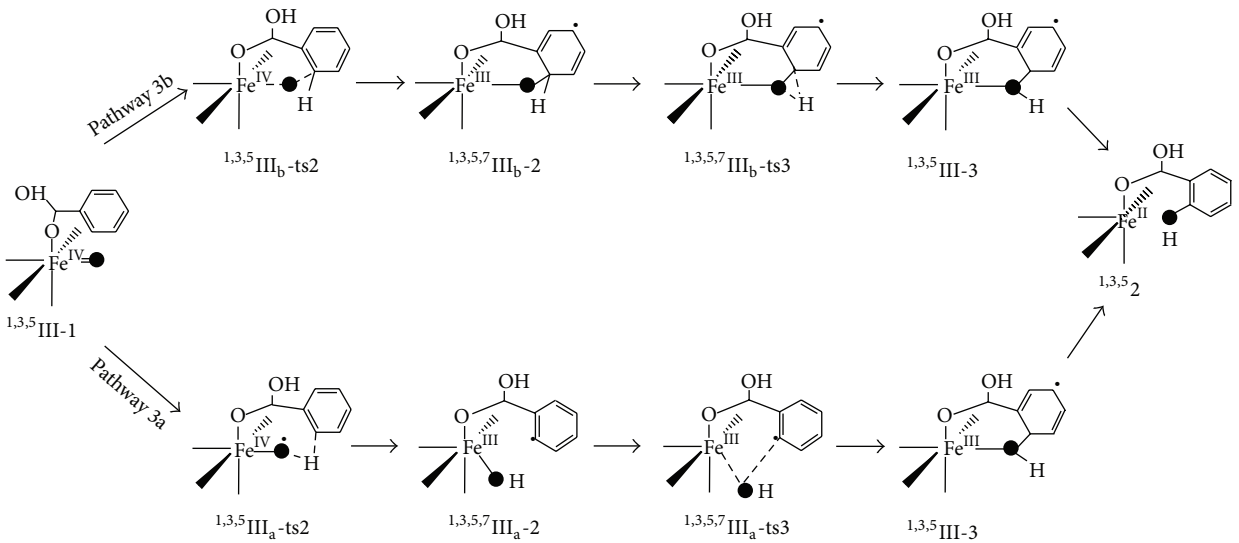

Figure 5: Schematic mechanism for the *ortho*-hydroxylation reaction by Fe^{IV}=O oxidant where reaction may be proceeded via either C–H activation or electrophilic way.

Dataset Item 14 (Spectra). This computed energy profile for *ortho*-hydroxylation by electrophilic attack (pathway II_b) by Fe^{V}=O oxidant is optimized with M06-2X function. The computed values (ΔG) are given in kJ/mol.

Dataset Item 15 (Spectra). This computed energy profile for heterolytic cleavage of O–O bond of *trans*-Fe^{III}–OOH is optimized with B3LYP function. The computed values (ΔG) are given in kJ/mol.

Dataset Item 16 (Spectra). This computed energy profile for heterolytic cleavage of O–O bond of *trans*-Fe^{III}–OOH is optimized with B3LYP-D function. The computed values (ΔG) are given in kJ/mol.

Dataset Item 17 (Spectra). This computed energy profile for heterolytic cleavage of O–O bond of *trans*-Fe^{III}–OOH is optimized with wB97XD function. The computed values (ΔG) are given in kJ/mol.

Dataset Item 18 (Spectra). This computed energy profile for heterolytic cleavage of O–O bond of *trans*-Fe^{III}–OOH is optimized with B97D function. The computed values (ΔG) are given in kJ/mol.

Dataset Item 19 (Spectra). This computed energy profile for *ortho*-hydroxylation by C–H bond activation (pathway III_a) by Fe^{IV}=O oxidant is optimized with B3LYP function. The computed values (ΔG) are given in kJ/mol.

Dataset Item 20 (Spectra). This computed energy profile for *ortho*-hydroxylation by C–H bond activation (pathway III_a) by Fe^{IV}=O oxidant is optimized with B3LYP-D function. The computed values (ΔG) are given in kJ/mol.

Dataset Item 21 (Spectra). This computed energy profile for *ortho*-hydroxylation by electrophilic attack (pathway III_b) by Fe^{IV}=O oxidant is optimized with B3LYP function. The computed values (ΔG) are given in kJ/mol.

Dataset Item 22 (Spectra). This computed energy profile for *ortho*-hydroxylation by electrophilic attack (pathway III_b) by Fe^{IV}=O oxidant is optimized with B3LYP-D function. The computed values (ΔG) are given in kJ/mol.

Dataset Item 23 (Spectra). This computed energy profile for a relax scan for the generation from *trans*-Fe^{III}–OOH complex is optimized with B3LYP function. The computed values (ΔG) are given in kJ/mol.

Dataset Item 24 (Spectra). This computed energy profile for a relax scan for the generation from *trans*-Fe^{III}–OOH complex is optimized with B3LYP-D function. The computed values (ΔG) are given in kJ/mol.

Dataset Item 25 (Table). Optimized coordinates by B3LYP functional.

Column 1: Structure
Column 2: Atom
Column 3: *X* Coordinate
Column 4: *Y* Coordinate
Column 5: *Z* Coordinate
Column 6: Attack Type

Dataset Item 26 (Table). Optimized coordinates of *trans* isomer of N-*cis* isomer by B3LYP functional.

Column 1: Structure
Column 2: Atom
Column 3: *X* Coordinate
Column 4: *Y* Coordinate
Column 5: *Z* Coordinate
Column 6: Attack Type

Dataset Item 27 (Table). Optimized coordinates by B3LYP-D functional.

Column 1: Structure
Column 2: Atom
Column 3: *X* Coordinate
Column 4: *Y* Coordinate
Column 5: *Z* Coordinate
Column 6: Attack Type

Dataset Item 28 (Table). Optimized coordinates by wB97XD functional.

Column 1: Structure
Column 2: Atom
Column 3: *X* Coordinate
Column 4: *Y* Coordinate
Column 5: *Z* Coordinate

Dataset Item 29 (Table). Optimized coordinates by B97D functional.

Column 1: Structure
Column 2: Atom
Column 3: *X* Coordinate
Column 4: *Y* Coordinate
Column 5: *Z* Coordinate

Dataset Item 30 (Table). Optimized coordinates by M06-2X functional.

Column 1: Structure
Column 2: Atom
Column 3: *X* Coordinate
Column 4: *Y* Coordinate
Column 5: *Z* Coordinate

4. Concluding Remarks

The presented exhaustive data offer one possible way to collect a dataset from theoretical modelling of reaction mechanisms where all the computed parameters for a particular reaction studied earlier are listed. The collection of dataset has a great advantage; apart from the fact that it can help verify the energies and structures, the mechanism of reactions can also be qualitatively predicted if the electronic structures of all the relevant species (reactant, intermediates, transition states, and products) are available.

Dataset Availability

The dataset associated with this Dataset Paper is dedicated to the public domain using the CC0 waiver and is available at http://dx.doi.org/10.1155/2014/753131/dataset.

Conflict of Interests

The authors declare that there is no conflict of interests regarding the publication of this paper.

Acknowledgments

Gopalan Rajaraman would like to acknowledge financial support from the Government of India through the Department of Science and Technology (SR/S1/IC-41/2010) and Indian Institute of Technology, Bombay, to access the high performance computing facility. Azaj Ansari would like to thank CSIR for a fellowship.

References

[1] R. A. Sheldon and J. K. Kochi, *Metal-Catalyzed Oxidations of Organic Compounds*, Academic Press, New York, NY, USA, 1981.

[2] T. Punniyamurthy, S. Velusamy, and J. Iqbal, "Recent advances in transition metal catalyzed oxidation of organic substrates with molecular oxygen," *Chemical Reviews*, vol. 105, no. 6, pp. 2329–2364, 2005.

[3] O. V. Makhlynets, P. Das, S. Taktak et al., "Iron-promoted *ortho*-and/or *ipso*-hydroxylation of benzoic acids with H_2O_2," *Chemistry: A European Journal*, vol. 15, no. 47, pp. 13171–13180, 2009.

[4] O. V. Makhlynets and E. V. Rybak-Akimova, "Aromatic hydroxylation at a non-heme iron center: observed intermediates and insights into the nature of the active species," *Chemistry: A European Journal*, vol. 16, no. 47, pp. 13995–14006, 2010.

[5] M. J. Park, J. Lee, Y. Sun, J. Kim, and W. Nam, "Reactivities of mononuclear non-heme iron intermediates including evidence that iron(III)−hydroperoxo species Is a sluggish oxidant," *Journal of the American Chemical Society*, vol. 128, no. 8, pp. 2630–2634, 2006.

[6] A. Bassan, M. R. A. Blomberg, P. E. M. Siegbahn, and L. Que Jr., "A density functional study on a biomimetic non-heme iron catalyst: insights into alkane hydroxylation by a formally HO–Fe^{V} = O oxidant," *Chemistry: A European Journal*, vol. 11, no. 2, pp. 692–705, 2005.

[7] A. Bassan, M. R. A. Blomberg, and P. E. M. Siegbahn, "Mechanism of aromatic hydroxylation by an activated Fe^{IV} = O core in tetrahydrobiopterin-dependent hydroxylases," *Chemistry: A European Journal*, vol. 9, no. 17, pp. 4055–4067, 2003.

[8] A. Thibon, V. Jollet, C. Ribal et al., "Hydroxylation of aromatics with the help of a non-haem FeOOH: a mechanistic study under single-turnover and catalytic conditions," *Chemistry: A European Journal*, vol. 18, no. 9, pp. 2715–2724, 2012.

[9] B. Meunier, "Metalloporphyrins as versatile catalysts for oxidation reactions and oxidative DNA cleavage," *Chemical Reviews*, vol. 92, no. 6, pp. 1411–1456, 1992.

[10] N. Kitajima, H. Fukui, and Y. Moro-oka, "A model for methane mono-oxygenase: dioxygen oxidation of alkanes by use of a μ-oxo binuclear iron complex," *Journal of the Chemical Society, Chemical Communications*, no. 7, pp. 485–486, 1988.

[11] J. B. Vincent, J. C. Huffman, G. Christou et al., "Modeling the dinuclear sites of iron biomolecules: synthesis and properties of $Fe_2O(OAc)_2Cl_2(bipy)_2$ and its use as an alkane activation catalyst," *Journal of the American Chemical Society*, vol. 110, no. 20, pp. 6898–6900, 1988.

[12] W. Nam and J. S. Valentine, "Hydroxylation of alkanes by hydrogen peroxide catalyzed by iron complexes in the presence of pyridine or 2,2'-bipyridine," *New Journal of Chemistry*, vol. 13, no. 10-11, pp. 677–682, 1989.

[13] R. A. Leising, R. E. Norman, and L. Que Jr., "Alkane functionalization by non-porphyrin iron complexes: mechanistic insights," *Inorganic Chemistry*, vol. 29, no. 14, pp. 2553–2555, 1990.

[14] F. T. de Oliveira, A. Chanda, D. Banerjee et al., "Chemical and spectroscopic evidence for an Fe^{V}-Oxo complex," *Science*, vol. 315, no. 5813, pp. 835–838, 2007.

[15] O. Y. Lyakin, K. P. Bryliakov, G. J. P. Britovsek, and E. P. Talsi, "EPR spectroscopic trapping of the active species of nonheme iron-catalyzed oxidation," *Journal of the American Chemical Society*, vol. 131, no. 31, pp. 10798–10799, 2009.

[16] A. R. McDonald and L. Que Jr., "Iron-oxo complexes: elusive iron(V) species identified," *Nature Chemistry*, vol. 3, no. 10, pp. 761–762, 2011.

[17] A. Ansari, A. Kaushik, and G. Rajaraman, "Mechanistic insights on the *ortho*-hydroxylation of aromatic compounds by non-heme iron complex: a computational case study on the comparative oxidative ability of ferric-hydroperoxo and high-valent Fe^{IV} = O and Fe^{V} = O intermediates," *Journal of American Chemical Society*, vol. 135, no. 11, pp. 4235–4249, 2013.

[18] M. J. Frisch, G. W. Trucks, H. B. Schlegel et al., *Revision 02*, Gaussian 09, Gaussian, Wallingford, Conn, USA, 2009.

[19] C. Lee, W. Yang, and R. G. Parr, "Development of the Colle-Salvetti correlation-energy formula into a functional of the electron density," *Physical Review B*, vol. 37, no. 2, pp. 785–789, 1988.

[20] A. D. Becke, "Density-functional thermochemistry. III. The role of exact exchange," *The Journal of Chemical Physics*, vol. 98, no. 7, pp. 5648–5652, 1993.

[21] T. H. Dunning, Jr, and P. J. Hay, in *Modern Theoretical Chemistry*, H. F. Schaefer III, Ed., vol. 3, pp. 1–28, Plenum, New York, NY, USA, 1976.

[22] P. J. Hay and W. R. Wadt, "*Ab initio* effective core potentials for molecular calculations. Potentials for the transition metal atoms Sc to Hg," *The Journal of Chemical Physics*, vol. 82, no. 1, pp. 270–283, 1985.

[23] W. R. Wadt and P. J. Hay, "*Ab initio* effective core potentials for molecular calculations. Potentials for main group elements Na to Bi," *The Journal of Chemical Physics*, vol. 82, no. 1, pp. 284–298, 1985.

[24] P. J. Hay and W. R. Wadt, "*Ab initio* effective core potentials for molecular calculations. Potentials for K to Au including the outermost core orbitale," *The Journal of Chemical Physics*, vol. 82, no. 1, pp. 299–310, 1985.

[25] R. Ditchfield, W. J. Hehre, and J. A. Pople, "Self-consistent molecular-orbital methods. IX. An extended gaussian-type basis for molecular-orbital studies of organic molecules," *The Journal of Chemical Physics*, vol. 54, no. 2, pp. 724–728, 1985.

[26] S. Shaik, H. Hirao, and D. Kumar, "Reactivity of high-valent iron-oxo species in enzymes and synthetic reagents: a tale of many states," *Accounts of Chemical Research*, vol. 40, no. 7, pp. 532–542, 2007.

[27] S. Kozuch and S. Shaik, "How to conceptualize catalytic cycles? the energetic Span model," *Accounts of Chemical Research*, vol. 44, no. 2, pp. 101–110, 2011.

[28] S. Shaik, D. Kumar, S. P. de Visser, A. Altun, and W. Thiel, "Theoretical perspective on the structure and mechanism of cytochrome P450 enzymes," *Chemical Reviews*, vol. 105, no. 6, pp. 2279–2328, 2005.

[29] P. E. M. Siegbahn and M. R. A. Blomberg, "Transition-metal systems in biochemistry studied by high-accuracy quantum chemical methods," *Chemical Reviews*, vol. 100, no. 2, pp. 421–438, 2000.

[30] E. I. Solomon, T. C. Brunold, M. I. Davis et al., "Geometric and electronic structure/function correlations in non-heme iron enzymes," *Chemical Reviews*, vol. 100, no. 1, pp. 235–350, 2000.

[31] S. Ye and F. Neese, "Nonheme oxo-iron(IV) intermediates form an oxyl radical upon approaching the C–H bond activation transition state," *Proceedings of the National Academy of Sciences of the United States of America*, vol. 108, no. 4, pp. 1228–1233, 2011.

[32] C. Greco, M. Bruschi, P. Fantucci, U. Ryde, and L. de Gioia, "Mechanistic and physiological implications of the interplay among iron-sulfur clusters in [FeFe]-hydrogenases. A QM/MM perspective," *Journal of the American Chemical Society*, vol. 133, no. 46, pp. 18742–18749, 2011.

[33] V. N. Staroverov, G. E. Scuseria, J. Tao, and J. P. Perdew, "Comparative assessment of a new nonempirical density functional: molecules and hydrogen-bonded complexes," *Journal of Chemical Physics*, vol. 119, no. 23, pp. 12129–12137, 2003.

[34] N. C. Handy and A. J. Cohen, "Left-right correlation energy," *Molecular Physics*, vol. 99, no. 5, pp. 403–412, 2001.

[35] M. Guell, J. M. Lius, M. Solà, and M. Swart, "Importance of the basis set for the spin-state energetics of iron complexes," *Journal of Physical Chemistry A*, vol. 112, no. 28, pp. 6384–6391, 2008.

[36] M. M. Conradie, J. Conradie, and A. Ghosh, "Capturing the spin state diversity of iron(III)-aryl porphyrins: OLYP is better than TPSSh," *Journal of Inorganic Biochemistry*, vol. 105, no. 1, pp. 84–91, 2011.

[37] Y. Zhao and D. G. Truhlar, "The M06 suite of density functionals for main group thermochemistry, thermochemical kinetics, noncovalent interactions, excited states, and transition elements: two new functionals and systematic testing of four M06-class functionals and 12 other functionals," *Theoretical Chemistry Accounts*, vol. 120, no. 1-3, pp. 215–241, 2008.

[38] S. Grimme, "Semiempirical GGA-type density functional constructed with a long-range dispersion correction," *Journal of Computational Chemistry*, vol. 27, no. 15, pp. 1787–1799, 2006.

[39] J.-D. Chai and M. Head-Gordon, "Long-range corrected hybrid density functionals with damped atom-atom dispersion corrections," *Physical Chemistry Chemical Physics*, vol. 10, no. 44, pp. 6615–6620, 2008.

[40] S. Grimme, "Accurate description of van der Waals complexes by density functional theory including empirical corrections," *Journal of Computational Chemistry*, vol. 25, no. 12, pp. 1463–1473, 2004.

[41] H. Chen, W. Lai, and S. Shaik, "Exchange-enhanced H-abstraction reactivity of high-valent nonheme iron(IV)-Oxo from coupled cluster and density functional theories," *The Journal of Physical Chemistry Letters*, vol. 1, no. 10, pp. 1533–1540, 2010.

[42] C. Møller and M. S. Plesset, "Note on an approximation treatment for many-electron systems," *Physical Review*, vol. 46, no. 7, pp. 618–622, 1934.

[43] F. Neese, "Theoretical spectroscopy of model-nonheme $\left[\mathrm{Fe\,(IV)\,OL_5}\right]^{2+}$ complexes in their lowest triplet and quintet states using multireference *ab initio* and density functional theory methods," *Journal of Inorganic Biochemistry*, vol. 100, no. 4, pp. 716–726, 2006.